Published in final edited form as:
Biochemistry. 2008 August 19; 47(33): 8600–8606. doi:10.1021/bi800687h.

Computationally Designed Peptide Inhibitors of Protein-Protein Interactions in Membranes

Gregory A. Caputo[§], **Rustem I. Litvinov**[†], **Wei Li**[‡], **Joel S. Bennett**[‡], **William F. DeGrado**[†], and **Hang Yin**[⊥,*]

[⊥] Department of Chemistry and Biochemistry, University of Colorado, Boulder, Colorado 80309-0215

[‡] Department of Cell and Developmental Biology, University of Pennsylvania School of Medicine, Philadelphia, Pennsylvania 19104

[‡] Hematology-Oncology Division, Department of Medicine, University of Pennsylvania School of Medicine, Philadelphia, Pennsylvania 19104

[†] Department of Biochemistry and Biophysics, University of Pennsylvania School of Medicine, Philadelphia, Pennsylvania 19104

Abstract

We recently reported a computational method (CHAMP) to design sequence-specific peptides that bind to the membrane-embedded portions of transmembrane proteins. We successfully applied this method to design membrane-spanning peptides targeting the transmembrane domains of the α_{IIb}-subunit of integrin $\alpha_{IIb}\beta_3$. Previously, we demonstrated that these CHAMP peptides bind specifically with reasonable affinity to isolated transmembrane helices of the targeted transmembrane region. These peptides also induced integrin $\alpha_{IIb}\beta_3$ activation due to disruption of the helix-helix interactions between the transmembrane domains of the α_{IIb} and β_3 subunits. In this paper, we show the direct interaction of the designed anti-α_{IIb} CHAMP peptide with isolated full-length integrin $\alpha_{IIb}\beta_3$ in detergent micelles. Further, the behavior of the designed peptides in phospholipid bilayers is essentially identical to their behavior in detergent micelles. In particular, the peptides assume a membrane-spanning α-helical conformation that does not disrupt bilayer integrity. The activity and selectivity of the CHAMP peptides was further explored in platelets, comfirming that anti-α_{IIb} activates wild type $\alpha_{IIb}\beta_3$ in whole cells as a result of its disruption of the protein-protein interactions between the α- and β-subunits at the transmembrane regions. These results demonstrate that CHAMP is a successful chemical biology approach that can provide specific tools to probe the transmembrane domains of proteins.

Keywords

membrane protein; protein-protein interactions; transmembrane domain; computational design; integrin

Membrane proteins account for approximately 30% of the entire human proteome; however, studies of their transmembrane (TM) domains have lagged behind due to limitation of their availability, the complexity of the model systems used to study membrane proteins (e.g. micelles, phospholipids vesicles, and bicelles), and in particular, the lack of exogenous probes

*Corresponding authors: E-mail: hang.yin@colorado.edu; Telephone: (303) 492 6786; Fax: (303) 492 5894.
[§]Current Address: Department of Chemistry and Biochemistry, Rowan University, Glassboro, New Jersey 08028-1701

with high affinity and specificity (1). Conventional antibody-based probing techniques are only useful for water-soluble regions of proteins. Currently, there is no widely used chemical biology method to specifically target the TM domains of proteins using exogenous agents.

Computational protein engineering has made major strides (2). There are now a variety of methods to design proteins that recognize water-soluble regions of target proteins (3–6), but few companion methods for targeting TM regions have been successful. Recently, we reported a general strategy for the computational design of TM domain-targeted peptides, designated the CHAMP (computed helical anti-membrane protein) method (7). We illustrated the utility of the method by designing peptides that specifically recognize the TM helix of the α-subunit of the platelet integrin $\alpha_{IIb}\beta_3$. The TM helices of the α and β subunits of integrin $\alpha_{IIb}\beta_3$ are thought to associate heteromerically in unstimulated platelets and to dissociate following platelet stimulation (8–10). We showed that anti-α_{IIb}, a peptide designed to target the α_{IIb} TM helix, activated $\alpha_{IIb}\beta_3$ by disrupting the heteromeric α_{IIb}/β_3 TM helix-helix interaction of the resting integrin (Figure 1). These results illustrate the potential of CHAMP method for generating high affinity molecules that bind to and modulate functions of membrane proteins.

In this paper, we validate the specificity of the anti-α_{IIb} CHAMP peptide, using biophysical methods to confirm that it recognizes full-length integrin $\alpha_{IIb}\beta_3$ in vitro and in living cells. We found that anti-α_{IIb} selectively binds to the isolated full-length integrin $\alpha_{IIb}\beta_3$ in detergent micelles and phospholipid bilayers, assumes a membrane-spanning α-helical conformation that does not disrupt the bilayer integrity, and activates $\alpha_{IIb}\beta_3$ by disrupting the association of α_{IIb} and β_3 transmembrane helices. These results support the notion that CHAMP is a general method for design membrane-spanning peptides targeting protein TM domains.

EXPREIMENTAL PROCEDURES

General Peptide Synthesis

Peptides were synthesized using an Applied Biosystems 430A peptide synthesizer at 0.25 mmole scales. These peptides were synthesized on a Rink Amide AM resin (200–400 mesh) (Nova Biochem) with a substitution level of 0.71 mmole/g. Activation of the free amino acids was achieved with 2-(1H-7-azabenzotriazol-1-yl)-1,1,3,3-tetramethyl uronium hexafluorophosphate methanaminium (HATU, 0.40 M solution in DMF). The reaction solvent contains 25% DMSO and 75% NMP (HPLC grade, Aldrich). Side chain deprotection and simultaneous cleavage from the resin was performed using a mixture of trifluoroacetic acid (TFA)/thioanisole/1,2-ethanedithiol/anisole (90:5:3:3 v/v) at room temperature, under N_2 flow for 2 hours. The crude peptides collected from precipitation with cold diethyl ether (Aldrich) were dissolved in a mixture of 2-propanol:acetonitrile: water (6:3:1) and then lyophilized overnight. The peptides were then purified on a preparative reverse phase HPLC system (Varian ProStar 210) with a C-4 preparative column (Vydac) using a linear gradient of buffer A (0.1% TFA in Millipore water) and buffer B (6:3:1 2-propanol: acetonitrile: water) containing 0.1% TFA. Elution of the purified peptides occurred at approximately 75% of buffer B. The identities of the purified peptides were confirmed by MALDI-TOF mass spectroscopy on a Voyager Biospectrometry Workstation (PerSeptive Biosystems), and their purity was assessed using HP1100 analytical HPLC system (Hewlett Packard) with an analytical C-4 column (Vydac) and a linear A/B gradient.

The coumarin label of anti-α_{IIb} and anti-α_{IIb}mut was attached using standard method (12). Two additional glycine residues were coupled to the amino terminal of the peptide-resin using standard manual peptide synthesis conditions. The Fmoc protection group was removed with 20% piperidine in DMF. Resin was rinsed with DMF four times then swelled with dichloromethane and drained. 7-Hydroxycoumarin-3-carboxylic acid (Anaspec) was dissolved in a mixture of pyridine/DMF/DCM (12:7:5) to prepare 0.1 M solution. The resulting solution

was added to the resin. The suspension mixture was stirred under room temperature in dark until the ninhydrin test indicates that the reaction is completed.

Sodium Dodecyl Sulfate Polyacrylamide Gel Electrophoresis (SDS-PAGE)

Electrophoresis was carried out using precast SDS polyacrylamide gels (12% NuPAGE 10-well Bis-Tris gels, Invitrogen). The peptide samples were prepared in buffer (10 mM HEPES (pH=7.5), 60 mM N-octyl-β-D- glucopyranoside, 0.5 mM $CaCl_2$, 0.02% NaN_3) and left incubated overnight. Before electrophoresis, each sample was incubated at 90°C for 7 min. Electrophoresis was carried out at room temperature with NuPAGE MES SDS running buffer (Invitrogen) at 125 mV for 55 minutes. The resulting gel was stained using NOVEX stain kit (Invitrogen).

Fluorescence Anisotropy Assay

The full-length integrin $\alpha_{IIb}\beta_3$ protein in buffer (7.9 mg/ml, 10 mM HEPES (pH=7.5), 60 mM N-octyl-β-D-glucopyranoside, 0.5 mM $CaCl_2$, 0.02% NaN_3) is prepared using the previously reported method (13). Fluorescence polarization experiments were conducted on an ATF105 spectrofluorometer (Aviv Instrument, Inc) using a 0.3 cm path length cuvette. Spectra were measured at 25 °C using 1.0 nm slit widths. Excitation at 408 nm was used for the coumarin-labeled peptide. Anisotropy measurements were recorded upon titration of the integrin $\alpha_{IIb}\beta_3$ protein at varying concentrations into a solution of 64 nM of the anti-α_{IIb} CHAMP peptide. Data analysis was carried out using previously described method (14).

Attenuated Total Reflection Infrared (ATR-IR) Spectroscopy

ATR-IR spectroscopy was performed as previously described (15). Briefly, the purified anti-α_{IIb} peptide was solubilized in a 1:1 (v:v) mixture of 2-propanol:H_2O containing 0.1% HCl, frozen, and lyophilized. This process was repeated for a total of 3 rounds to remove any TFA salts from the purification process. The anti-α_{IIb} peptide was then solubilized in a 1:1 (v:v) mixture of 2-propanol:H_2O, mixed with an appropriate volume of lipid dissolved in $CHCl_3$, and dried under a stream of N_2. The lipid composition was a mixture of 1- palmitoyl-2-oleoyl-*sn*-glycero-3-phosphocholine (POPC) and 1-palmitoyl-2-oleoyl-*sn*-glycero-3- [phospho-*rac*-(1-glycerol)] (POPG) (7:3 mol:mol). The final peptide:lipid ratio in the sample was 1:50. The dried peptide-lipid film was subjected to high vacuum for 2–3 hours to remove any traces of solvent. The film was reconstituted in 5 mM HEPES buffered D_2O at ~pH 7.1 by vigorous vortexing. The peptide-lipid suspension was then extruded 17 times using an Avestin liposofast mini extruder (Avestin Inc.) equipped with 2 stacked polycarbonate membranes with average pore diameter of 200 nm. The peptide-containing vesicles were deposited on the ATR crystal, gently spread with a Teflon bar to form a film, and dried under a gentle stream of N_2. Infrared spectra were recorded on a Nicolet 4700 infrared spectrophotometer (Thermo-Electron Corp.) equipped with a DTGS detector, a ZnSe wire-grid polarizer, and a home built flow chamber to allow a stream of N_2 bubbled through D_2O to flow over the sample during collection. The internal reflection element was a zinc-selenide ATR crystal (80 × 20 × 3 mm) with an angle of 45° yielding 25 internal reflections. A total of 512 scans at polarizations of 0° and 90° were collected for each sample. Spectra were recorded at 2 cm^{-1} resolution and analyzed using the OMNIC software package for peak deconvolution and area analysis. Helix orientation angle was calculated from the spectra as previously described (16) with the exception that the value used in this study for the crystal refractive index was 2.42 (ZnSe).

Dye Release Assay

Lipids were purchased from Avanti Polar Lipids Inc. (Alabaster, Al) and used without further purification. Formation of large unilamellar vesicles with entrapped $Tb(DPA)_3$ was performed as previously described with several modifications (17). POPC and POPG dissolved in

chloroform were mixed (7:3 mol:mol) with a trace amount of L-3-phosphatidylcholine-1,2-di [^{14}C]oleoyl (Amersham Biosciences). The lipid mixture was initially dried under a stream of N_2, then further dessicated under vacuum for at least 3 hours to remove any residual chloroform. The dried lipid film was then stored under a head of N_2 at −20°C until used. To form liposomes, the lipid film was rehydrated in HBS buffer (10mM HEPES, 100mM NaCl, pH 7.1) containing 5mM $TbCl_3$ (Molecular Probes, a division of Invitrogen, Carlsbad, CA) and 15mM 2,6-pyridinedicarboxylic acid (DPA, Sigma-Aldrich, neutralized to pH 7.0) to obtain a final lipid concentration of 20mM (typically a final volume of 0.5 ml was used). The sample was vigorously vortexed for at least 3 minutes to ensure complete resuspension of the lipid film. The sample was then subjected to 7 rounds of freezing in a dry-ice/acetone bath and thawed at 37°C, to increase trapping yield. The sample was then passed 21 times through a Liposofast extruder (Avestin Inc., Ottowa, Canada) with two stacked polycarbonate membranes, each with a pore size of 200nm. Liposomes were then separated from untrapped molecules by gel filtration on a Sepharose CL-2B column (Sigma, 1.0 cm i.d. × 22cm). Lipid concentration was calculated by measuring radioactivity in liposome containing fractions after the column with a comparison to the radioactivity in an aliquot of liposomes that was taken before the gel filtration step. Liposomes were stored at 4°C and used for up to 1 week after preparation. Each liposome preparation was checked for nonspecific leakage before use by monitoring fluorescence in the absence of any externally added analytes.

An aliquot of $Tb(DPA)_3$-containing liposomes were added to HBS supplemented with 10mM EDTA for a final concentration of 20 μM total lipid in 1700 μl volume. Samples were allowed to equilibrate for approximately 5 minutes at which point initial intensity readings were taken (F_0). Peptides (or controls) were then added to the sample from a concentrated stock in DMSO to obtain the desired peptide:lipid ratio and allowed to equilibrate for 10 minutes with constant stirring at which point emission intensity was again recorded (F). Leakage was normalized to the fluorescence intensity value for complete vesicle disruption induced by addition of detergent (F_M).

Hemolysis Assay

The hemolytic effects of the anti-α_{IIb} and anti-α_{IIb}mut peptides were tested using previously described method (18). Suspension of human erythrocytes (RBC, 1 %) with peptides of different concentrations were incubated in 150 mM sodium chloride and 10 mM Tris buffer (pH= 7.0), in the presence or absence of 1 mg/ml bovine serum albumin (BSA). The samples were prepared by combining 400 mL of the RBC suspension and peptide stock solutions (10 mM in DMSO). After incubation at 37°C for 1 h, the samples were centrifuged at 14 000 rpm for 5 min, and the OD_{400} of the supernatant was measured.

Transmission Electron Microscopy (TEM)

Electron microscopy of purified integrin $\alpha_{IIb}\beta_3$ heterodimers was performed as previously described (19). Rotary-shadowed samples were prepared using a modification of standard procedures (20) by spraying a dilute solution of molecules in a volatile buffer (0.05 M ammonium formate) and glycerol (30–50%) onto freshly-cleaved mica and shadowing with tungsten in a vacuum evaporator (Denton Vacuum Co., Cherry Hill, NJ). All specimens were examined in a FEI/Philips 400 electron microscope (Philips Electronic Instruments Co., Mahwah, NJ), operating at 80 kV and at a magnification of 60,000 ×.

Fluorescence-Activated Cell Sorting (FACS)

Freshly isolated platelets were added to 200 mg/ml FITC-conjugated fibrinogen, then incubated with 20 μM ADP or 2 μM the anti-α_{IIb} CHAMP peptides in presence or absence of 5 mM EDTA for 3 minutes at room temperature. After incubation, the platelets were fixed with

0.37% formalin in PBS buffer for 10 minutes, then washed and examined by FACS analysis as previously reported (21).

RESULTS AND DISCUSSION

Anti-α_{IIb} was prepared using Fmoc solid-state peptide synthesis (SSPS) with HATU as the activating agent to overcome the difficulty of synthesizing membrane-embed protein sequences (22). Double coupling conditions were used at the β-branched amino acid residues. High purity was confirmed by chromatography. A control peptide, anti-α_{IIb}mut, in which the three Gly residues in the "Gly zipper" motif (GXXXGXXXG) were mutated to Leu (23), was also synthesized, as was a peptide, designated α_{IIb}-TM, spanning residues Trp968 to Lys989 of α_{IIb} (Figure 2A). For binding measurements using fluorescence spectroscopy, we prepared 7-hydroxycoumarin-3-carboxamide-labeled anti-α_{IIb} (coum- anti-α_{IIb}) and anti-α_{IIb}mut (coum-anti-α_{IIb}mut) via a linker to the N-termini of the peptides.

To confirm that the designed CHAMP peptides, as well as its target α_{IIb}-TM, take up structured conformations in artificial membrane systems (detergent micelles) and undergo oligomerization as previously reported in cellular membranes (7,24), we used SDS-PAGE to study the oligomerization state of the free and tagged anti-α_{IIb} peptides as well as anti-α_{IIb}mut. SDS has previously been shown to provide a micellar environment that mimicks phospholipid bilayers (25). We found that both anti-α_{IIb} (M.W.=3.7 kD) and coumarin-labelled anti-α_{IIb} (M.W.=4.0 kD) migrated as dimers (Figure 2B), consistent with previous experiment using the TOXCAT system that measures transmembrane domain interactions in bacterial membranes (7). By contrast, anti-α_{IIb}mut migrated as a monomer, confirmed that the Gly zipper motif is critical for the inter-helical recognition. Taken together, these results indicate that detergent micelles are a valid model system to study CHAMP peptide/target interactions. They also demonstrate that CHAMP peptides have high propensity to homo-dimerize, even in the presence of excessive competing detergent molecules.

Previously, we found that anti-α_{IIb} associates with a short peptide (M.W.= ca. 3 kD) corresponding to the TM region of the α_{IIb}-subunit of integrin $\alpha_{IIb}\beta_3$ in micelles and phospholipid vesicles (7). However, $\alpha_{IIb}\beta_3$ is a complex macromolecule (MW= ca. 230 kD) containing two non-identical transmembrane domains. To demonstrate that anti-α_{IIb} also binds to the α_{llb} transmembrane domain in full-length $\alpha_{IIb}\beta_3$, we used fluorescence anisotropy titrations of anti-α_{IIb} to full-length $\alpha_{IIb}\beta_3$ in N-octyl-β-D-glucopyranoside micelles. The fluorescence anisotropy of a coumarin-labeled peptide in solution correlates with its tumbling and rotational rates (14). However, when bound to the much larger protein, its tumbling is constrained and polarization increases. The advantages of this assay are that it does not require immobilization of either the receptor or the ligand, requires small amounts of peptide and protein as fluorescein has high quantum yield, and can be readily developed into a high-throughput format. We added increasing amounts of coumarin-labeled anti-α_{IIb} or anti-α_{IIb}mut to a constant concentration of $\alpha_{IIb}\beta_3$ solution and monitored the resulting polarization increase. Plotting the anisotropy of coum-anti-α_{IIb} as a function of the concentration of $\alpha_{IIb}\beta_3$ revealed a binding isotherm with an apparent K_{diss} of $1.3\pm0.2 \times 10^{-5}$ in mole fraction units, indicating that the peptide also binds tightly to the intact integrin (Figure 3). The control peptide, coum-anti-α_{IIb}mut, displayed an ≈ 100-fold lower affinity for $\alpha_{IIb}\beta_3$. We also found that coum-anti-α_{IIb} specifically recognized the TM domain of intergrin α_{IIb}, but not that of intergrin α_v, demonstrating that these CHAMP peptides can differentiate closely relevant homologous integral membrane targets (7).

Integrins are inactive when their TM domain-containing stalks are in proximity and active when the stalks separate (19,26). Consistent with our previous report, transmission electron microscopy (TEM) of purified rotary shadowed $\alpha_{IIb}\beta_3$ in buffer containing N-octyl-β-D-

glucopyranoside and 1 mM $CaCl_2$ revealed that the majority of inactive $\alpha_{IIb}\beta_3$ molecules had a closed configuration with their stalks touching at the their tips (19). By contrast, when anti-α_{IIb} was present, most of the $\alpha_{IIb}\beta_3$ molecules had an open configuration with separated stalks. Statistical analyses indicated that the presence of 5.0 μM anti-α_{IIb} induced the majority of integrin $\alpha_{IIb}\beta_3$ molecules to convert to its active form (Figure 4). By contrast, anti-α_{IIb}mut induced negligible activation under the same concentrations. These observations are consistent with the notion that anti-α_{IIb} activates $\alpha_{IIb}\beta_3$ by disrupting the TM heterodimer maintaining the integrin in its inactive state.

To demonstrate that anti-α_{IIb} takes up a membrane-spanning orientation in phospholipid bilayers, we used phospholipid vesicles as the artificial membrane system and polarized attenuated total reflection infrared (ATR-IR) spectroscopy to confirm that anti-α_{IIb} spans the membrane. ATR-IR spectroscopy exploits the fact that in an ordered sample, a given bond will absorb infrared radiation differentially depending on the polarization of the light and the angle at which the bond is oriented relative to the polarized light. If the secondary structure of a peptide is known, the dichroic ratio (R^{ATR}) of the amide-I absorbance when the incident light is polarized at 0° to the amide-I absorbance when the light is polarized at 90° can be used to calculate the angle between the helical axis of the peptide and the bilayer normal. We observed the position of the amide-I vibration at 1656 cm^{-1}, indicating that anti-α_{IIb} adopted primarily an α-helical conformation in the POPC/POPG bilayers, consistent with the previously published CD data (Fig. 5). The R^{ATR} of 4.7 corresponds to an angle ~20°, indicating that the peptide was inserted nearly perpendicular to the plane of the bilayer. The ~20° angle of insertion is not surprising considering the 33 amino acid length of the peptide, which, if completely helical, would form an α-helix of ~49Å. This is somewhat longer than the hydrophobic thickness of the POPC/POPG bilayer core and could result in peptide tilting to compensate for the hydrophobic mismatch. The representative spectra of the methylene stretching region of the polarized ATR-IR spectra of POPC/POPG bilayers in the absence and in the presence of anti-α_{IIb} are shown in Figure 5C. The dichroic ratios (R^{ATR}) values calculated from this region of the spectra are indicative of bilayer ordering, as the major signal arises from the symmetric (~2850cm^{-1}) and asymmetric (~2920cm^{-1}) stretching of the -CH_2- groups in the lipid acyl chains (27,28). The comparison between the PCPG/PCPG bilayers with and without anti-α_{IIb} showed only a small difference in the dichroic ratios, indicating that the peptide is not significantly disrupting the internal organization of the bilayer or the ability of the bilayers to stack into multilayers on the ZnSe crystal (27).

Because amphiphilic peptides can cause cell lysis (29), we examined the ability of anti-α_{IIb} to permeabilize phospholipid membranes. Anti-α_{IIb} did not induce significant leakage of a fluorescent metal complex, $Tb(DPA)_3$, from lipid vesicles at lipid/peptide ratio up to 10:1 suggesting that the anti-α_{IIb} peptide does not significantly perturb the cell membrane (Fig. 6). Further toxicity tests for these compounds were conducted using a lactate dehydrogenase (LDH) release assay. Platelets release LDH when their plasma membrane is perturbed. In the presence of 10 μM of anti-α_{IIb}, the level of LDH released by platelets is not significantly higher than the negative control. Moreover, anti--α_{IIb} did not lyse human erythrocyte membranes at the concentrations up to 10 μM.

Agonist-stimulated platelets undergo rapid $\alpha_{IIb}\beta_3$-dependent aggregation in response to agonists such as ADP when the plasma protein fibrinogen binds to the activated conformation of $\alpha_{IIb}\beta_3$ (30). To directly demonstrate whether anti-α_{IIb} induces the active conformation of $\alpha_{IIb}\beta_3$ in intact platelets, we used fluorescence-activated cell sorting (FACS) to measure FITC-labeled fibrinogen binding to platelets. The difference in agonist-stimulated fibrinogen binding in presence and absence of the calcium chelator EDTA indicated the amount of fibrinogen specifically bound to $\alpha_{IIb}\beta_3$. As shown in Figure 7, 2.0 μM anti-α_{IIb} induced ≈ 50% as much specific FITC-fibrinogen binding to platelets as did platelet stimulation by 20 μM ADP. By

contrast, anti-α_{IIb}mut showed little ability to induce fibrinogen binding to platelets (data not shown). Thus, these data indicate that although not as potent a stimulus at ADP, anti-α_{IIb} does directly enable $\alpha_{IIb}\beta_3$ to bind fibrinogen.

In summary, these results validate the CHAMP method as a successful general chemical biology approach to provide molecular probes with high affinity and specificity for membrane-embedded segments of proteins. In particular, the CHAMP peptide, anti-α_{IIb}, provides a specific tool for addressing the role of TM domain association in regulating the function of the integrin $\alpha_{IIb}\beta_3$. By blocking the site on the α_{IIb} TM helix that engages the β_3 helix, anti-α_{IIb} activates the integrin, providing strong support for the hypothesis that separation of the helices is required for activation (10). CHAMP peptides provide a route to molecules that bind TM regions of their targets, expanding the range of conventional antibody-based methods that can only be applied to water-soluble regions of proteins. Given the current interests involving studying the lateral TM helix associations in membrane protein folding, assembly, and signal transduction (31), CHAMP peptides may provide much-needed reagents for probing these processes. Last, although hurdles (such as poor solubility in aqueous solution) associated with the physical properties of the peptides need to be overcome, it is encouraging that engineered peptides from TM helices have shown promises in animal models (32,33). The CHAMP peptides can serve as lead sequences for the development of more drug-like, small-molecule peptidomimetic inhibitors of membrane protein-protein interactions, which might ultimately find applications as clinical diagnostics or therapeutics.

Acknowledgments

This work was supported by NIH grants GM60610, GM54616, HL40387, and HL81012. H.Y. thanks financial supports from the University of Colorado, the Association for Research of Childhood Cancer, and the Sidney Kimmel Foundation for Cancer Research (SKF-08-101).

ABBREVIATIONS

ADP
adenosine diphosphate

ATR-IR
attenuated total reflection infrared

BSA
bovine serum albumin

CHAMP
computed helical anti-membranef protein

DMF
Dimethylformamide

DMSO
dimethyl sulfoxide

HATU
2-(1H-7-azabenzotriazol-1-yl)-1,1,3,3-tetramethyl uronium hexafluorophosphate methanaminium

EDTA
ethylenediaminetetraacetic acid

DPA

dipicolinic acid

FACS
fluorescence activated cell sorting

FITC
fluorescein isothiocyanate

LDH
lactate dehydrogenase

NMP
N-Methyl-Pyrrolidine

POPC
1-palmitoyl-2-oleoyl-*sn*-glycero-3-phosphocholine

POPG
1-palmitoyl-2-oleoyl-*sn*-glycero-3-[phospho-*rac*-(1-glycerol)]

RBC
human erythrocytes

SDS-PAGE
sodium dodecyl sulfate polyacrylamide gel electrophoresis

TEM
transmission electron microscopy

TFA
trifluoroacetic acid

TFE
2,2,2-trifluoroethanol

TM
transmembrane

References

1. Yin H. Exogenous Agents that Target Transmembrane Domains of Proteins. Angew Chem Int Ed 2008;47:2744–2752.
2. Kang SG, Saven JG. Computational protein design: structure, function and combinatorial diversity. Curr Opin Chem Biol 2007;11:329–334. [PubMed: 17524729]
3. Kortemme T, Baker D. Computational design of protein-protein interactions. Curr Opin Chem Biol 2004;8:91–97. [PubMed: 15036162]
4. Shifman JM, Mayo SL. Exploring the origins of binding specificity through the computational redesign of calmodulin. Proc Natl Acad Sci U S A 2003;100:13274–13279. [PubMed: 14597710]
5. Reina J, Lacroix E, Hobson SD, Fernandez-Ballester G, Rybin V, Schwab MS, Serrano L, Gonzalez C. Computer-aided design of a PDZ domain to recognize new target sequences. Nat Struct Biol 2002;9:621–627. [PubMed: 12080331]
6. Ogihara NL, Ghirlanda G, Bryson JW, Gingery M, DeGrado WF, Eisenberg D. Design of three-dimensional domain-swapped dimers and fibrous oligomers. Proc Natl Acad Sci U S A 2001;98:1404–1409. [PubMed: 11171963]
7. Yin H, Slusky JS, Berger BW, Walters RS, Vilaire G, Litvinov RI, Lear JD, Caputo GA, Bennett JS, DeGrado WF. Computational design of peptides that target transmembrane helices. Science 2007;315:1817–1822. [PubMed: 17395823]

8. Partridge AW, Liu SC, Kim S, Bowie JU, Ginsberg MH. Transmembrane domain helix packing stabilizes integrin $\alpha_{IIb}\beta_3$ in the low affinity state. J Biol Chem 2005;280:7294–7300. [PubMed: 15591321]
9. Luo BH, Springer TA, Takagi J. A specific interface between integrin transmembrane helices and affinity for ligand. Plos Biol 2004;2:776–786.
10. Li W, Metcalf DG, Gorelik R, Li RH, Mitra N, Nanda V, Law PB, Lear JD, DeGrado WF, Bennett JS. A push-pull mechanism for regulating integrin function. Proc Natl Acad Sci U S A 2005;102:1424–1429. [PubMed: 15671157]
11. Wegener KL, Partridge AW, Han J, Pickford AR, Liddington RC, Ginsberg MH, Campbell ID. Structural basis of integrin activation by talin. Cell 2007;128:171–182. [PubMed: 17218263]
12. http://www.anaspec.com.
13. Weisel JW, Nagaswami C, Vilaire G, Bennett JS. Examination of the platelet membrane glycoprotein IIb-IIIa complex and its interaction with fibrinogen and other ligands by electron microscopy. J Biol Chem 1992;267:16637–16643. [PubMed: 1644841]
14. Yin H, Lee GI, Park HS, Payne GA, Rodriguez JM, Sebti SM, Hamilton AD. Terphenyl-based helical mimetics that disrupt the p53/HDM2 interaction. Angew Chem Int Ed 2005;44:2704–2707.
15. Caputo GA, London E. Cumulative effects of amino acid substitutions and hydrophobic mismatch upon the transmembrane stability and conformation of hydrophobic alpha-helices. Biochemistry 2003;42:3275–3285. [PubMed: 12641459]
16. Arkin IT, MacKenzie KR, Brunger AT. Site-directed dichroism as a method for obtaining rotational and orientational constraints for oriented polymers. J Am Chem Soc 1997;119:8973–8980.
17. Heuck AP, Tweten RK, Johnson AE. Assembly and topography of the prepore complex in cholesterol-dependent cytolysins. J Biol Chem 2003;278:31218–31225. [PubMed: 12777381]
18. Liu D, DeGrado WF. De novo design, synthesis, and characterization of antimicrobial beta-peptides. J Am Chem Soc 2001;123:7553–7559. [PubMed: 11480975]
19. Litvinov RI, Nagaswami C, Vilaire G, Shuman H, Bennett JS, Weisel JW. Functional and structural correlations of individual $\alpha_{IIb}\beta_3$ molecules. Blood 2004;104:3979–3985. [PubMed: 15319287]
20. Weisel JW, Stauffacher CV, Bullitt E, Cohen C. A model for fibrinogen: domains and sequence. Science 1985;230:1388–1391. [PubMed: 4071058]
21. Basani RB, D'Andrea G, Mitra N, Vilaire G, Richberg M, Kowalska MA, Bennett JS, Poncz M. RGD-containing peptides inhibit fibrinogen binding to platelet $\alpha_{IIb}\beta_3$ by inducing an allosteric change in the amino-terminal portion of α_{IIb}. J Biol Chem 2001;276:13975–13981. [PubMed: 11278919]
22. Fisher LE, Engelman DM. High-yield synthesis and purification of an α-helical transmembrane domain. Anal Biochem 2001;293:102–108. [PubMed: 11373085]
23. Kim S, Jeon TJ, Oberai A, Yang D, Schmidt JJ, Bowie JU. Transmembrane glycine zippers: physiological and pathological roles in membrane proteins. Proc Natl Acad Sci U S A 2005;102:14278–14283. [PubMed: 16179394]
24. Yin H, Litvinov RI, Vilaire G, Zhu H, Li W, Caputo GA, Moore DT, Lear JD, Weisel JW, Degrado WF, Bennett JS. Activation of platelet $\alpha_{IIb}\beta_3$ by an exogenous peptide corresponding to the transmembrane domain of α_{IIb}. J Biol Chem 2006;281:36732–36741. [PubMed: 17032655]
25. DeGrado WF, Gratkowski H, Lear JD. How do helix-helix interactions help determine the folds of membrane proteins? Perspectives from the study of homo-oligomeric helical bundles. Protein Sci 2003;12:647–665. [PubMed: 12649422]
26. Kim M, Carman CV, Springer TA. Bidirectional transmembrane signaling by cytoplasmic domain separation in integrins. Science 2003;301:1720–1725. [PubMed: 14500982]
27. Torrecillas A, Martínez-Senac MM, Goormaghtigh E, de Godos A, Corbalán-García S, Gómez-Fernández JC. Modulation of the membrane orientation and secondary structure of the C-terminal domains of Bak and Bcl-2 by lipids. Biochemistry 2005;44:10796–10809. [PubMed: 16086582]
28. Goormaghtigh E, Raussens V, Ruysschaert JM. Attenuated total reflection infrared spectroscopy of proteins and lipids in biological membranes. Biochim Biophys Acta 1999;1422:105–185. [PubMed: 10393271]
29. Bechinger B. Structure and functions of channel-forming peptides: Magainins, cecropins, melittin and alamethicin. J Membr Biol 1997;156:197–211. [PubMed: 9096062]

30. Bennett JS. Novel platelet inhibitors. Annu Rev Med 2001;52:161–184. [PubMed: 11160773]
31. Senes A, Engel DE, DeGrado WF. Folding of helical membrane proteins: the role of polar, GXXXG-like and proline motifs. Curr Opin Struct Biol 2004;14:465–479. [PubMed: 15313242]
32. Manolios N, Collier S, Taylor J, Pollard J, Harrison LC, Bender V. T-cell antigen receptor transmembrane peptides modulate T-cell function and T cell-mediated disease. Nat Med 1997;3:84–88. [PubMed: 8986747]
33. Gerber D, Quintana FJ, Bloch I, Cohen IR, Shai Y. D-enantiomer peptide of the TCR alpha transmembrane domain inhibits T-cell activation in vitro and in vivo. FASEB J 2005;19:1190–1192. [PubMed: 15837719]

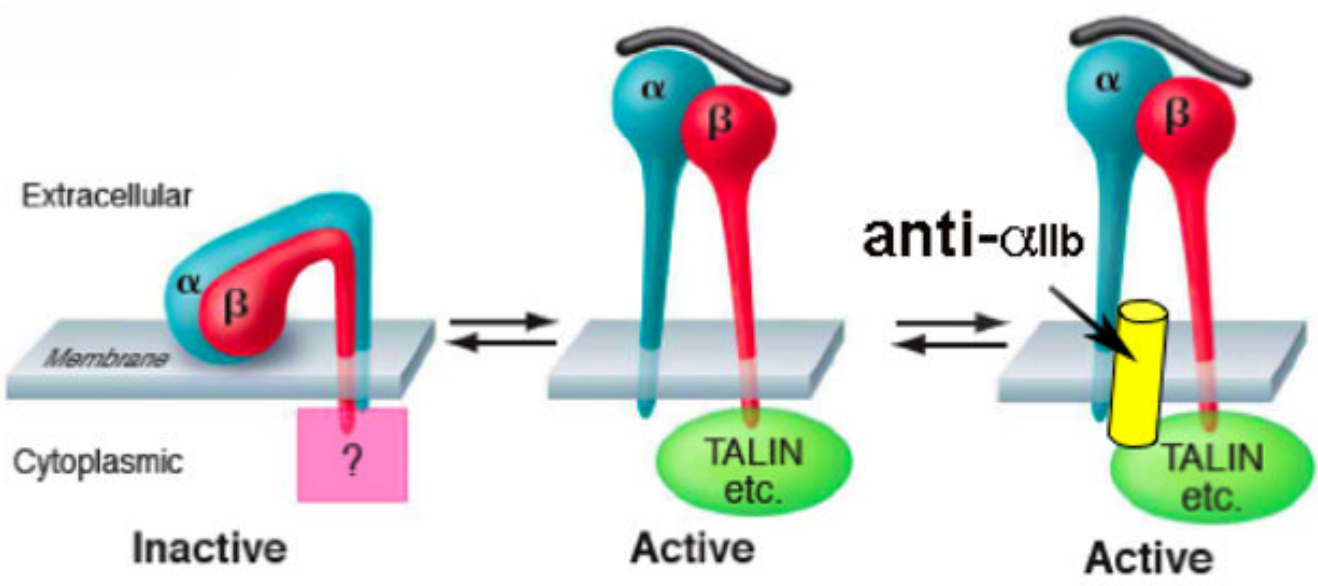

FIGURE 1.

Schematic diagram of integrin $\alpha_{IIb}\beta_3$ regulation. Because the α_{IIb} and β_3 subunit TM domains interact when integrins are inactive, any process that destabilizes this interaction would be expected to allow dissociation of the TM domains with concomitant integrin activation. In platelets, this occurs when platelets are stimulated by agonists such as adenosine diphosphate (ADP), inducing binding of the talin phosphotyrosine-binding domain to integrin β_3-subunit cytoplasmic domains (11). CHAMP peptides activate platelets by blocking the interactions between the TM helices of the α- and β-subunits of integrin $\alpha_{IIb}\beta_3$. Extracellular ligands for integrin $\alpha_{IIb}\beta_3$ (e.g. fibrinogen) are shown in black tubes. Question marks indicate unclear interactions.

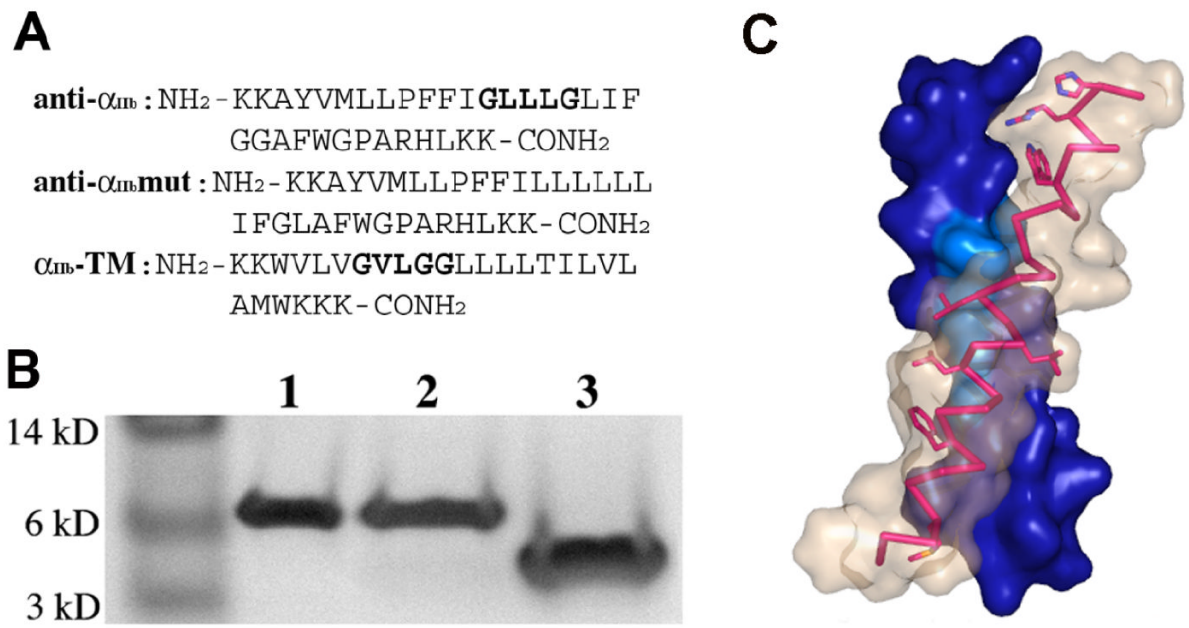

FIGURE 2.

(A) Sequences of the anti-α_{IIb} CHAMP peptide, the control peptide anti-α_{IIb}mut, and the targeted α_{IIb}-TM helix; (B) SDS-PAGE of anti-α_{IIb} (**1**), coumarin-labeled anti-α_{IIb} (**2**), and anti-α_{IIb}mut (**3**). (C) Computational model of anti-a_{IIb} bound to the α_{IIb} TM domain. The model predicts that anti-α_{IIb} (red stick) recognizes the "hot spot" on the α_{IIb}-TM binding surface (light blue) with spatial complementarity at the helix-crossing site.

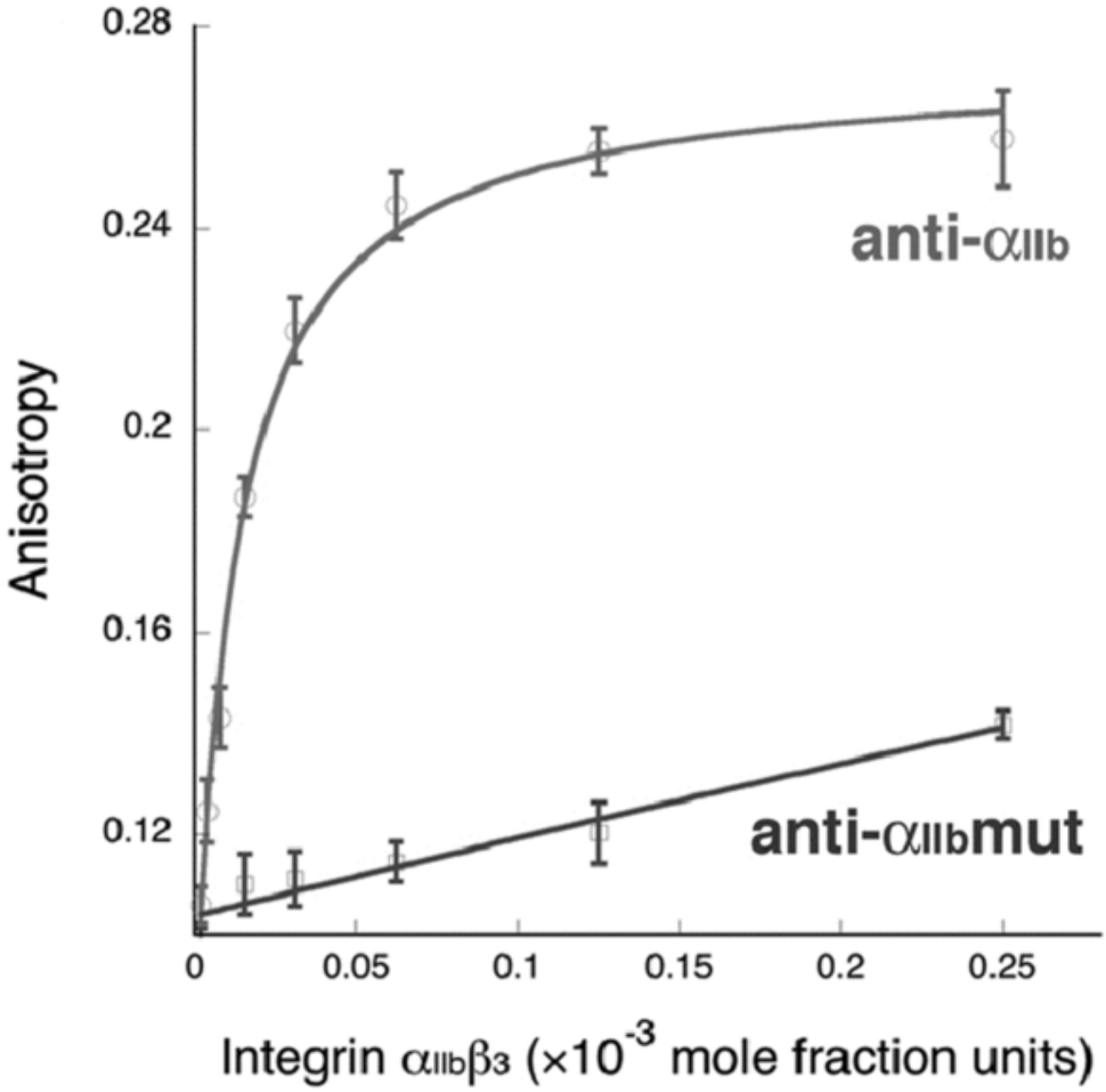

FIGURE 3.
Fluorescence polarization titration shows that full-length integrin $\alpha_{IIb}\beta_3$ selectively associates with anti-α_{IIb} over anti-α_{IIb}mut.

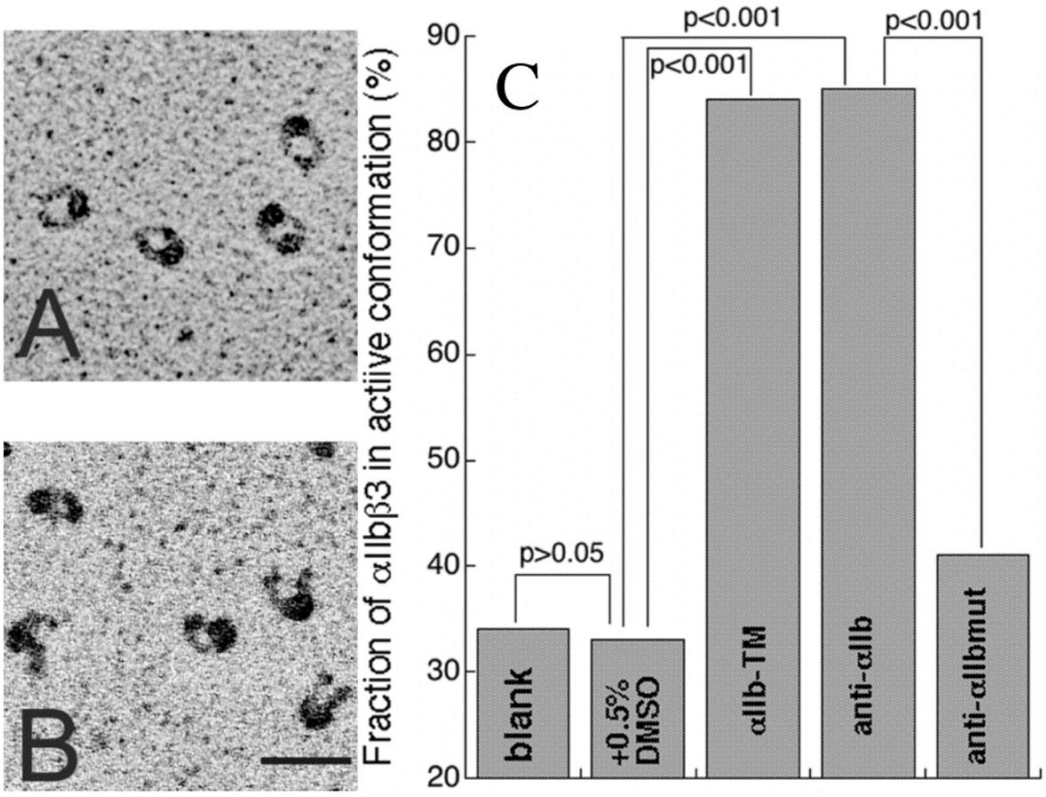

FIGURE 4.

Transmission electron microscopy of purified $\alpha_{IIb}\beta_3$ in "closed", (A, $CaCl_2$-containing buffer alone) and "open" (B, in $CaCl_2$-containing buffer + 3 μM anti-α_{IIb}) forms. Individual $\alpha_{IIb}\beta_3$ molecules were visualized using TEM after rotary shadowing with tungsten (magnification 170,000×; magnification bar = 30 nm). Integrin molecules are found either in the inactive or active state with their transmembrane stalks close and open, respectively. (C) Statistical analyses of the effects of α_{IIb}–TM, anti-α_{IIb}, and anti-α_{IIb}mut in activating integrin $\alpha_{IIb}\beta_3$.

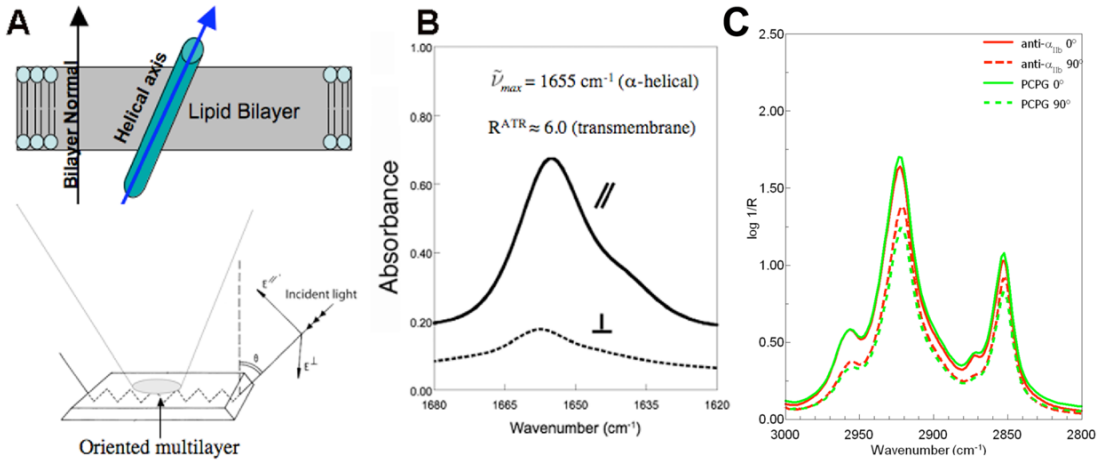

FIGURE 5.

ATR-IR (A) Schematic representation of ATR-IR experiments. Helix angle with respect to the bilayer normal is calculated using the ratio of the AmideI absorbance band using 0° and 90° polarized incident radiation, R^{ATR}; (B) ATR-IR spectra collected at 0° (//) and 90° (⊥) polarized incident radiation. (C) The methylene stretching region of the polarized ATR-IR spectra of POPC/POPG bilayers in the absence (green) and in the presence (red) of anti-α_{IIb}. The average R^{ATR} for pure POPC/POPG lipid bilayers was ~1.45 while the R^{ATR} for bilayers containing anti-α_{IIb} was ~1.33 (R^{ATR} values are averages of 2–3 independent samples).

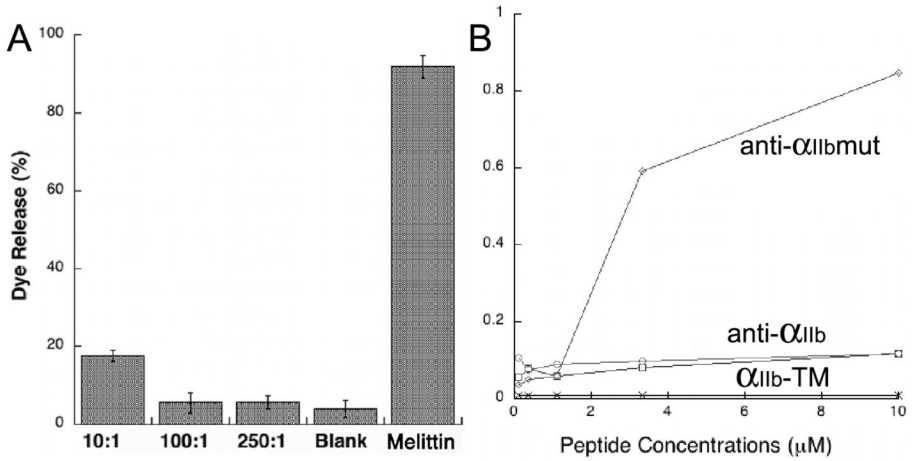

FIGURE 6.

Toxicity assays. (A) Dye release induced by anti-α_{IIb}. POPC:POPG (7:3) vesicles containing trapped Tb and DPA were exposed to anti-α_{IIb} at various peptide/lipid ratios or to the known pore-forming peptide melittin. Peptides were incubated with the loaded vesicles for 10 minutes before fluorescence was measured. Release was quantified using intensity before addition as a baseline (F_0) and fluorescence after the vesicles had been completely disrupted with detergent as a final maximum fluorescence (F_M). (B) Hemolysis induced by the CHAMP peptides. Human erythrocyte hemolysis induced by increasing concentrations of anti-α_{IIb} (circle), α_{IIb}-TM (square), and anti-α_{IIb}mut (diamonds) in 10 mM Tris buffer (pH= 7.0), 1mg/mL BSA.

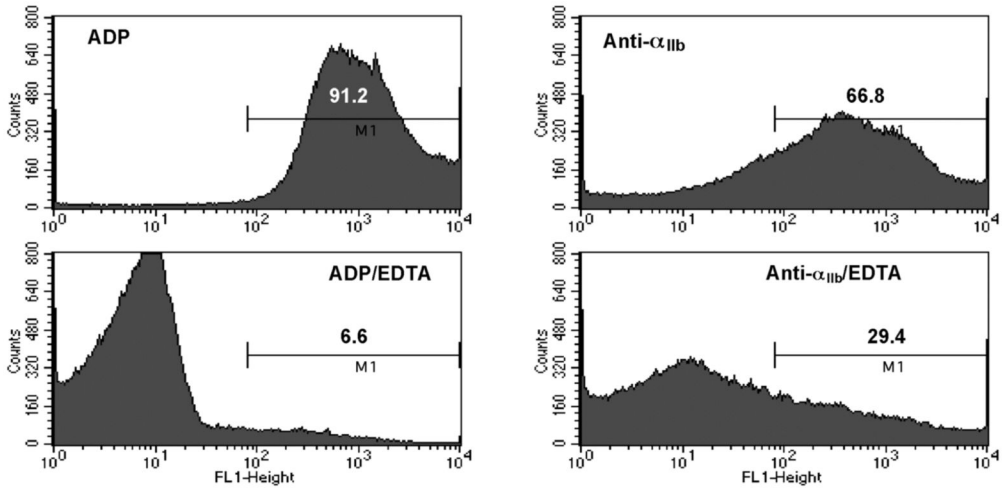

FIGURE 7.

Measurement of anti-α_{IIb}-induced binding of FITC-fibrinogen to gel-filtered human platelets by flow cytometry. Fibrinogen binding stimulated by (Top Left) 20 μM ADP, (Top Right) 2 μM anti- α_{IIb}; (Bottom Left) 20 μM ADP in the presence of 5 mM EDTA, and (Bottom Right) 2 μM anti-α_{IIb} in the presence of 5 mM EDTA. The numbers above M1 represent the percent of analyzed platelets present in the gate.